Thermoelectric properties of chalcogenide based $Cu_{2+x}ZnSn_{1-x}Se_4$

Ch. Raju, M. Falmbigl, P. Rogl, X. Yan, E. Bauer, J. Horky, M. Zehetbauer, and Ramesh Chandra Mallik'

Citation: AIP Advances **3**, 032106 (2013); doi: 10.1063/1.4794733
View online: http://dx.doi.org/10.1063/1.4794733
View Table of Contents: http://aip.scitation.org/toc/adv/3/3
Published by the American Institute of Physics

Thermoelectric properties of chalcogenide based $Cu_{2+x}ZnSn_{1-x}Se_4$

Ch. Raju,[1] M. Falmbigl,[2] P. Rogl,[2] X. Yan,[3] E. Bauer,[3] J. Horky,[4] M. Zehetbauer,[4] and Ramesh Chandra Mallik[1,a]
[1]*Department of Physics, Indian Institute of Science, Bangalore 560012, India*
[2]*Institute of Physical Chemistry, University of Vienna, Währingerstrasse 42, A-1090 Wien, Austria*
[3]*Institute of Solid State Physics, TU Vienna, Wiedner Hauptstrasse 8-10, A-1040 Wien, Austria*
[4]*Research Group Physics of Nanostructures Materials, University of Vienna, Boltzmanngasse 5, A-1090 Wien, Austria*

(Received 31 December 2012; accepted 20 February 2013; published online 1 March 2013)

Quaternary chalcogenide compounds $Cu_{2+x}ZnSn_{1-x}Se_4$ ($0 \leq x \leq 0.15$) were prepared by solid state synthesis. Rietveld powder X-ray diffraction (XRD) refinements combined with Electron Probe Micro Analyses (EPMA, WDS-Wavelength Dispersive Spectroscopy) and Raman spectra of all samples confirmed the stannite structure (Cu_2FeSnS_4-type) as the main phase. In addition to the main phase, small amounts of secondary phases like ZnSe, CuSe and SnSe were observed. Transport properties of all samples were measured as a function of temperature in the range from 300 K to 720 K. The electrical resistivity of all samples decreases with an increase in Cu content except for $Cu_{2.1}ZnSn_{0.9}Se_4$, most likely due to a higher content of the ZnSe. All samples showed positive Seebeck coefficients indicating that holes are the majority charge carriers. The thermal conductivity of doped samples was high compared to $Cu_2ZnSnSe_4$ and this may be due to the larger electronic contribution and the presence of the ZnSe phase in the doped samples. The maximum $zT = 0.3$ at 720 K occurs for $Cu_{2.05}ZnSn_{0.95}Se_4$ for which a high-pressure torsion treatment resulted in an enhancement of zT by 30% at 625 K. [http://dx.doi.org/10.1063/1.4794733]

I. INTRODUCTION

Quaternary compounds (I_2-II-IV-VI_4) are promising materials for solar cell applications due to their suitable direct band gap E_g ($E_g = 1.44$ eV for $Cu_2ZnSnSe_4$ and $E_g = 0.98$ eV for $Cu_2CdSnSe_4$) and high absorption coefficient for wave numbers around 10^5 cm^{-1}.[1] Additionally, these compounds can also be used in thermoelectric devices, which can convert thermal energy into electrical energy and vice–versa. The efficiency of a thermoelectric (TE) device depends on a material parameter defined as a dimensionless thermoelectric figure of merit $zT = (S^2\sigma/\lambda)$ T, where S, σ, T and λ represent the Seebeck coefficient, electrical conductivity, absolute temperature and total thermal conductivity, respectively. The total thermal conductivity is composed of an electronic (λ_{el}) and a phonon contribution (λ_{ph}). There have been many attempts to improve zT of skutterudite, clathrate materials etc.[2] by applying Slack's PGEC (Phonon Glass Electron Crystal) concept[3] to their complex crystal structures. These PGEC materials possess high electrical conductivity and at the same time low thermal conductivity like a glass. Recently there has been considerable interest in studying the thermoelectric properties of wide band gap quaternary compounds, because conventional TE materials exhibit a narrow band gap in which a bipolar effect may reduce the thermoelectric efficiency.

[a]Corresponding author: Email: rcmallik@physics.iisc.ernet.in Tel: +9180-2293 2450.

Also, these compounds (e.g. $Cu_2ZnSnSe_4$) have complex crystal structures, which follow the concept of two structural/functional units:[4] a Cu_2Se_4 tetrahedral array acting as an electrically conducting unit and the other $ZnSnSe_4$ tetrahedral array acting as an insulating path. These compounds are like PGEC materials such as filled skutterudites, because the electrically insulating $ZnSnSe_4$ layer (which plays the role of filler atoms in skutterudites) responsible for low thermal conductivity is inserted between two electrically conducting Cu_2Se_4 layers (plays a role as the charge carrying network in skutterudites) accountable for high electrical conductivity.[5] Furthermore, these compounds (I_2-II-IV-VI_4) have been derived from binary II_4-VI_4 compounds with four unit cells using the concept of cross substitution (replacement of II_4 by two I, one II and one IV group element, respectively) and maintaining the ratio of the number of valence electrons to the number of atoms present in the compound as four.[6] This exhibits a naturally distorted structure and may lead to a decrease in thermal conductivity.[7] The improvement of zT can be obtained by enhancing electrical conductivity through doping /partial substitution and a high Seebeck coefficient because of their wide band gap and low thermal conductivity due to a naturally distorted crystal structure.[4,7] A significant improvement of the zT of bulk quaternary compounds like $Cu_2ZnSnSe_4$, $Cu_2CdSnSe_4$, $Cu_2ZnGeSe_4$ and nanostructured $Cu_2CdSnSe_4$, $Cu_2ZnGeSe_4$ through doping/partial substitution using the above concept has already been reported.[4,5,7–11] The maximum value of zT observed for bulk materials such as $Cu_{2.1}Zn_{0.9}SnSe_4$, $Cu_{2.1}Cd_{0.9}SnSe_4$, $Cu_2ZnSn_{0.9}In_{0.1}Se_4$ and $Cu_{2.075}Zn_{0.925}GeSe_4$ reached 0.91 at 860 K,[4] 0.65 at 700 K,[5] 0.95 at 850 K[7] and 0.45 at 670 K,[8] respectively. The nanostructured compounds $Cu_2CdSnSe_4$, $Cu_{2.15}Cd_{0.85}SnSe_{3.9}$, $Cu_{2.15}Zn_{0.85}GeSe_{3.9}$ and non-stoichiometric $Cu_2ZnSnSe_4$ when using a chemical synthesis route showed peak zT values 0.65 at 723 K,[9] 0.71 at 685 K,[10] 0.55 at 723 K[11] and 0.44 at 723 K,[12] respectively. Though the thermoelectric properties of the quaternary chalcogenides have been studied as above mentioned, there is no literature on phase purity and micro structural information on these compounds.

In this investigation, the authors synthesized the compounds $Cu_{2+x}ZnSn_{1-x}Se_4$ (with x = 0, 0.025, 0.050, 0.750, 0.100, 0.125, 0.150) through partial substitution of Cu for Sn, which is supposed to create more charge carriers and conducting pathways to improve the electrical conductivity by using the concept described above. A systematic study of the structural, phase purity and compositional analysis followed by thermoelectric properties of the prepared compounds $Cu_{2+x}ZnSn_{1-x}Se_4$ (with x = 0, 0.025, 0.050, 0.750, 0.100, 0.125, 0.150) is presented.

Two of the resulting samples were treated by a high-pressure torsion (HPT) process introducing additional structural defects and grain boundaries via severe plastic deformation. The influence of the HPT-treatment on the thermoelectric properties was studied.

II. EXPERIMENTAL DETAILS

The stoichiometric compounds $Cu_{2+x}ZnSn_{1-x}Se_4$ (x = 0, 0.025, 0.05, 0.75, 0.1, 0.125, 0.15) were prepared (about 10 g each) by a standard solid state synthesis method from ingots of starting materials (Cu 99.9999% Alfa Aesar, Zn 99.99% Sigma Aldrich, Sn 99.99% Sigma Aldrich, Se 99.999% Alfa Aesar), followed by sealing in quartz ampoules under a high vacuum of 10^{-2} Pa. All the samples were slowly heated up to 1170 K and kept at this temperature for 6 hrs. Then the samples were allowed to cool down to 773 K within 24 hrs, followed by subsequent annealing at 773 K for 172 hrs.

The ingots were crushed to a particle size below 500 μm in an argon-filled glove box (O_2-, H_2O-content < 15 ppm) and transferred to WC-ball mill containers with WC-balls. The ball milling procedure was carried out in a high-energy planetary mill (Vario Pulverisette 4). The resulting powders were transferred into graphite dies and hot pressed in an argon atmosphere at 773 K at a pressure of 56 MPa in a HP W 200/250-2200-200-KS (FCT Systeme GmbH). The high-pressure torsion process was carried out using a device from W. Klement, Austria, equipped with an inductive heating coil and an infrared pyrometer. Sample discs with a diameter of 10 mm and a height of ~1 mm were exposed to a temperature of 573 K and one revolution at a pressure of 4 GPa. The densities of the hot-pressed as well as the HPT-deformed samples were determined using Archimedes' principle. After ball milling and hot pressing, all the measured densities were at least >97% of the x-ray density. The HPT-treatment did not result in any detectable change of the sample density.

TABLE I. Nominal composition, hot pressing conditions, relative densities, WDS phase composition and secondary phase for $Cu_{2+x}ZnSn_{1-x}Se_4$ ($0 \leq x \leq 0.125$), hot pressed at 773 K, 56 MPa.

Nominal composition	Relative density, [%]	WDS, [at%]				WDS, composition[a]	Secondary Phases[b]	ZnSe volume fraction (%)
		Cu	Zn	Sn	Se			
$Cu_2ZnSnSe_4$	99.6	27.9	11.4	11.2	49.3	$Cu_{2.23}Zn_{0.91}Sn_{0.90}Se_{3.94}$	ZnSe; SeSn	0.45
$Cu_{2.025}ZnSn_{0.975}Se_4$	98.4	25.9	13.2	11.6	49.1	$Cu_{2.07}Zn_{1.05}Sn_{0.92}Se_{3.93}$	ZnSe	1.7
$Cu_{2.05}ZnSn_{0.95}Se_4$	98.1	25.9	11.8	12.5	49.5	$Cu_{2.07}Zn_{0.95}Sn_{1.00}Se_{3.96}$	ZnSe	0.75
$Cu_{2.075}ZnSn_{0.925}Se_4$	98.2	25.5	12.3	12.1	50.0	$Cu_{2.04}Zn_{0.98}Sn_{0.96}Se_{4.00}$	ZnSe	1.95
$Cu_{2.1}ZnSn_{0.9}Se_4$	97.5	26.8	12.0	11.7	49.3	$Cu_{2.14}Zn_{0.97}Sn_{0.94}Se_{3.94}$	ZnSe	10.04
$Cu_{2.125}ZnSn_{0.875}Se_4$	97.7	26.1	11.3	12.4	50.0	$Cu_{2.09}Zn_{0.91}Sn_{0.99}Se_{4.00}$	ZnSe; CuSe	2.54
$Cu_{2.15}ZnSn_{0.85}Se_4$	97.5	25.6	11.8	12.1	50.3	$Cu_{2.05}Zn_{0.95}Sn_{0.97}Se_{4.03}$	ZnSe; CuSe	2.1

[a]System internal standard pure elements were used for calibration.
[b]detected by WDS measurement.

All the samples were characterized by powder X-ray diffraction (XRD) after annealing and hot pressing by employing a Guinier-Huber Imaging plate system with $CuK_{\alpha 1}$-radiation as well as by electron probe microanalysis (EPMA) (Zeiss Supra 55 VP, 20 kV, EDX-detector (Oxford Instr.) and (JEOL JXA-8530F wavelength dispersive spectrometer (WDS)). Lattice parameters were determined by XRD using Si (a = 0.5431065 nm) as an internal standard. Crystallographic phase characterization was carried out using Rietveld refinement.[13] High temperature XRD patterns of $Cu_{2+x}ZnSn_{1-x}Se_4$ ($0 \leq x \leq 0.15$) samples were collected by a Bruker D8 Advance X-ray diffractometer using Cu K_α radiation and a Ta strip for heating.

Unpolarized Raman spectra of $Cu_{2+x}ZnSn_{1-x}Se_4$ ($0 \leq x \leq 0.125$) samples were recorded in the wave number range from 50 to 500 cm^{-1} at room temperature using a HORIBA Jobin Yvon LabRAM HR800 spectrometer equipped with an argon laser (514.5 nm).

Measurements of electrical resistivities and Seebeck-coefficients from 300 K to 700 K were carried out on an ULVAC ZEM 3-system. Thermal conductivity was evaluated from thermal diffusivity and heat capacity data collected with an ANTER Flashline 3000 unit in the same temperature range. The measurement errors for the electrical resistivity and the Seebeck coefficient are 5% and 10% for the thermal conductivity.

III. RESULTS AND DISCUSSION

A. Structural characterization and phase composition

XRD-patterns of the annealed as well as the hot pressed samples revealed the presence of the stannite phase for all the samples of $Cu_{2+x}ZnSn_{1-x}Se_4$ ($0 \leq x \leq 0.15$) crystallizing in a tetragonal crystal structure isotypic with the structure of Cu_2FeSnS_4. In all the samples the presence of ZnSe as a secondary phase was confirmed mainly by WDS measurements and partially by X-ray patterns. In addition to the ZnSe phase, a CuSe phase was detected in the case of the two samples $Cu_{2+x}ZnSn_{1-x}Se_4$ (x = 0.125,0.15) with the highest nominal Cu-content indicating the exceeding of the solubility limit, whereas the undoped sample revealed SnSe as an additional secondary phase (see Table I). The presence of ZnSe, SnSe in the sample with nominal composition $Cu_2ZnSnSe_4$ may be due to the deviation from its stoichiometry confirmed byWDS. The doping of Sn on Cu site in $Cu_2ZnSnSe_4$ leads to the off stoichiometry in the nominal composition of the compounds, which further may lead to the instability of the crystal structure. The existence of non-stoichiometry in these compounds may cause an increase in ZnSe phase with increase in Cu content. The $Cu_2ZnSnSe_4$ stannite structure is a derivative of the ZnSe-structure (sphalerite-type). In the chalcopyrite structure ($CuFeS_2$-type) the alternate ordering of Fe and Cu atoms on the cationic sublattice causes a doubling of the unit cell in c-direction and therefore a reduction to tetragonal symmetry. Although similar lattice geometry exists, in the stannite structure the three different elements

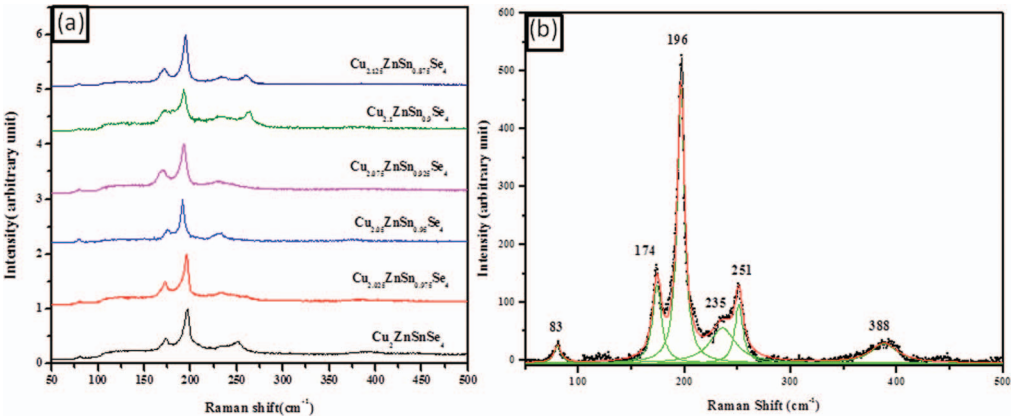

FIG. 1. (a) Raman spectra of $Cu_{2+x}ZnSn_{1-x}Se_4$ with $0 \leq x \leq 0.125$, (b) Raman spectrum with Lorentzian fitting $Cu_2ZnSnSe_4$.

TABLE II. Nominal composition, presence of stannite phase Raman modes including secondary phase modes such as ZnSe and CuSe for $Cu_{2+x}ZnSn_{1-x}Se_4$ ($0 \leq x \leq 0.125$).

Nominal composition	Mode1 (cm^{-1})	Mode2 (cm^{-1})	Mode3 (cm^{-1})	Mode4 (cm^{-1})	ZnSe vibrational mode (cm^{-1})	CuSe vibrational mode (cm^{-1})	Mode5 (cm^{-1})
$Cu_2ZnSnSe_4$	80.34	174.09	196.5	235.7	251.2		388
$Cu_{2.025}ZnSn_{0.975}Se_4$	80.5	173.7	195.7	235.9		258.2	380.2
$Cu_{2.05}ZnSn_{0.95}Se_4$	79.9	176.3	191.9	231.5			376.4
$Cu_{2.075}ZnSn_{0.925}Se_4$	79.8	170.5	192.9	229.5			
$Cu_{2.1}ZnSn_{0.9}Se_4$	80.2	172.6	193.4	233.5		263.6	384.2
$Cu_{2.125}ZnSn_{0.875}Se_4$	80.0	172.1	194.8	234.2		261.0	

Mode1-Mode5 represents the vibrational modes belonging to $Cu_2ZnSnSe_4$.

occupying the cationic sublattice are arranged in a different manner. The ratio of the lattice parameters *a*/*c* is very close to 0.5 and thus the splitting of several reflections is rather weak and hardly resolved. Moreover overlapping with the peaks of the ZnSe-phase (with very close lattice parameter *a* = 0.5664(1) nm)[14] is observed in most patterns and does not allow a proper determination of the ZnSe-content from XRD. In order to disentangle the contributions of both phases a complementary technique, Raman spectroscopy, was employed. Raman spectra of samples $Cu_{2+x}ZnSn_{1-x}Se_4$ ($0 \leq x \leq 0.125$) including a Lorentzian fitting for the Raman spectrum of $Cu_2ZnSnSe_4$ are shown in Figure 1. The results from Raman spectroscopy essentially confirm the information extracted by XRD and WDS as for all samples the corresponding peaks of the $Cu_2ZnSnSe_4$ phase were observed [see Table II], confirming the stannite structure to be the main phase.[15] In addition, a secondary phase peak related to ZnSe in the sample $Cu_2ZnSnSe_4$ and a peak of the CuSe phase in $Cu_{2+x}ZnSn_{1-x}Se_4$ ($x = 0.025, 0.1, 0.125$) were observed [see Table II]. The amount of the ZnSe phase was estimated only from the backscattered electron micrographs. In all the cases except for the sample with nominal composition $Cu_{2.1}ZnSn_{0.9}Se_4$ (ZnSe >10%) the amount of the ZnSe-phase is below 3%, and SnSe as well as CuSe impurities are less than 2% as documented by XRD as well as WDS data [see Table I]. In general, there is a unit cell volume decrease with increasing Cu-content, as both *a* and *c* slightly decrease (Fig. 2). Figure 3 shows the back-scattered electron micrographs of $Cu_2ZnSnSe_4$ and $Cu_{2.1}ZnSn_{0.9}Se_4$ in which the dark regions correspond to the secondary ZnSe phase. The sample compositions derived from WDS-data are listed in Table I. Due to the very small changes in the nominal composition no clear conclusion on the substitution of Sn by Cu in $Cu_{2+x}ZnSn_{1-x}Se_4$ can be extracted from XRD, Raman-Spectroscopy, and WDS. High temperature XRD measurements for all samples were carried out at temperatures of 300 K, 723 K, 748 K, and 773 K respectively. No structural changes were observed (see Fig. 4 for the representative sample $Cu_{2.05}ZnSn_{0.95}Se_4$). The thermal expansion coefficients calculated from the lattice parameters *a* and *c* range at

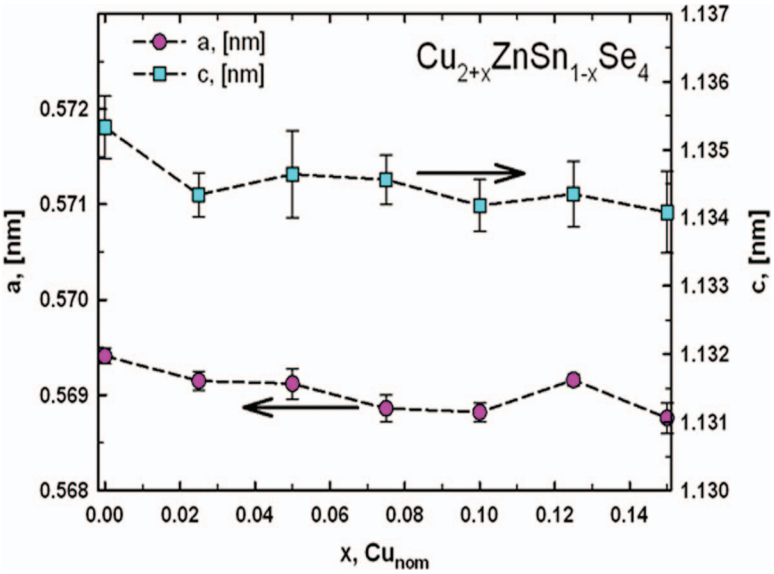

FIG. 2. Lattice parameters a and c as a function of the nominal Cu-content for $Cu_{2+x}ZnSn_{1-x}Se_4$ ($0 \leq x \leq 0.15$).

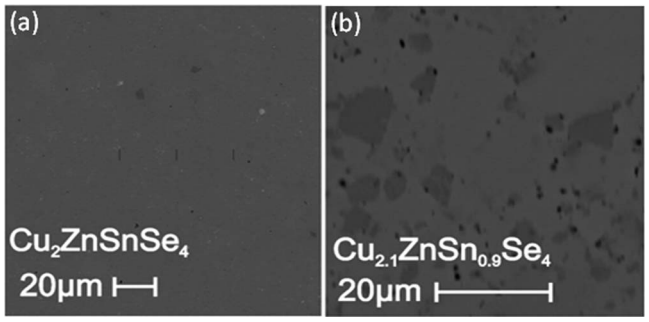

FIG. 3. (a, b) Back scattered electron micrographs of $Cu_2ZnSnSe_4$ and $Cu_{2.1}ZnSn_{0.9}Se_4$. The dark regions correspond to the secondary ZnSe-phase.

11.3×10^{-6} K^{-1} in the temperature interval from RT to 773 K [see Table III]. The only observable change in the powder patterns was the appearance of two small peaks at 26.28° and 43.56° in 2θ, which were successfully indexed with the high temperature modification of Cu_2Se (Pearson symbol: cF44, transition at 130 °C).[16]

Here the main interest is to give the possible explanation for the impact of secondary phases on transport properties of the main phase. The ZnSe secondary phase has an adverse effect on the transport properties as compared with other secondary phases because of the presence of the high ZnSe content in all the samples.

B. Transport properties

The temperature dependent electrical resistivity of all the samples above 300 K is plotted in Fig. 5. The electrical resistivity decreases with an increasing amount of Cu-doping, except for the sample $Cu_{2.1}ZnSn_{0.9}Se_4$ ($\rho_{300K} = 2664 \times 10^{-6}$ Ω cm), which is attributed to the significantly higher content of the secondary ZnSe-phase ($\rho_{300K} = 4.16 - 30.1$ Ω cm for bulk)[17] and ($\rho = 175 - 5$ Ω cm in between 300 K and 500 K for thin film)[18] and also may be due to higher scattering of holes with the ZnSe phase. The effect of SnSe and CuSe on the electrical resistivity is almost negligible because of their low resistivities (i.e, 0.169–0.176 Ω cm between 300 K and 780 K for SnSe,[19] 0.2 − 0.1 Ω cm between 300 K and 350 K for CuSe)[20] as compared with the electrical resistivity of

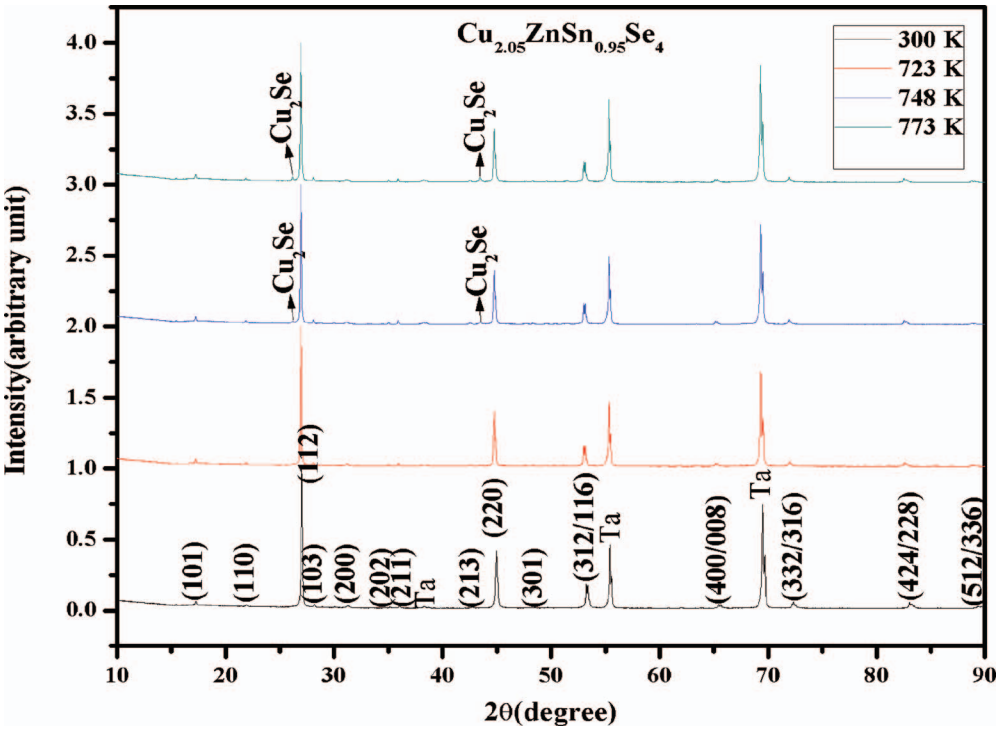

FIG. 4. High temperature x-ray powder patterns for sample $Cu_{2.05}ZnSn_{0.95}Se_4$.

TABLE III. Nominal composition, temperature, and lattice parameters for $Cu_{2+x}ZnSn_{1-x}Se_4$ ($0 \leq x \leq 0.125$).

Nominal composition	Temperature(K)	Lattice parameters, [nm]	
		A	*c*
$Cu_2ZnSnSe_4$	300	0.5694	1.1353
	723	0.5717	1.1407
	773	0.5721	1.1412
$Cu_{2.025}ZnSn_{0.975}Se_4$	300	0.5691	1.1343
	723	0.5717	1.1401
	773	0.5723	1.1408
$Cu_{2.05}ZnSn_{0.95}Se_4$	300	0.5691	1.1346
	723	0.5716	1.1400
	773	0.5720	1.1403
$Cu_{2.075}ZnSn_{0.925}Se_4$	300	0.5688	1.1346
	723	0.5716	1.1400
	773	0.5719	1.1404
$Cu_{2.1}ZnSn_{0.9}Se_4$	300	0.5688	1.1342
	723	0.5716	1.1398
	773	0.5718	1.1401
$Cu_{2.125}ZnSn_{0.875}Se_4$	300	0.5691	1.1344
	723	0.5716	1.1399
	773	0.5718	1.1402
$Cu_{2.15}ZnSn_{0.85}Se_4$	300	0.5687	1.1340
	723	0.5717	1.1401
	773	0.5719	1.1405

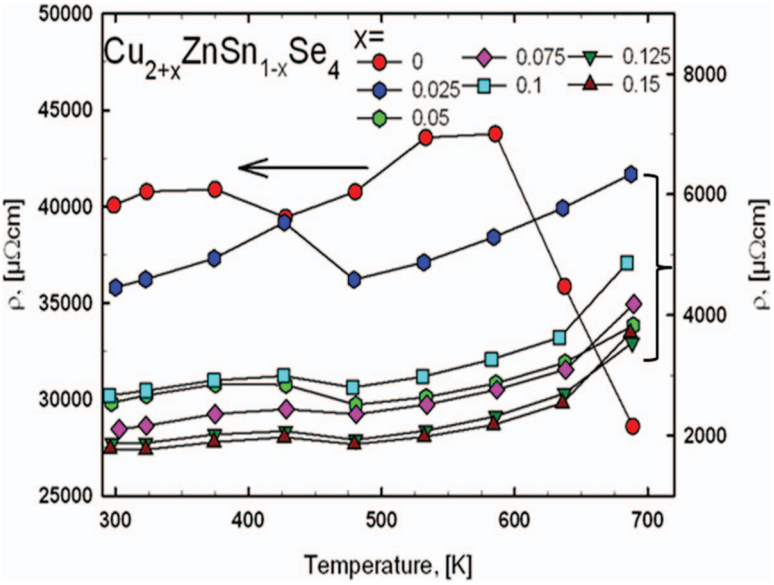

FIG. 5. Electrical resistivity as a function of temperature for $Cu_{2+x}ZnSn_{1-x}Se_4$ ($0 \leq x \leq 0.15$).

ZnSe. All the doped samples exhibit a maximum in ρ(T) between 300 K and 480 K followed by an increase of electrical resistivity with temperature. This maximum is not related to a structural change of the main phase as confirmed by high-TXRD. Only the undoped sample ($Cu_{nom} = 2$), exhibiting a much higher absolute electrical resistivity, shows a reverse trend. The room temperature values of electrical resistivity are decreasing dramatically for the samples $Cu_{2+x}ZnSnSe_4$ with $0 \leq x_{nom} \leq 0.05$ by almost 94%. The samples with a higher nominal Cu-content show a comparatively smaller change by a further decrease of 30%. Comparing the room temperature values of the electrical resistivity and Seebeck coefficient of $Cu_2ZnSnSe_4$ (nominal composition) with the literature data also demonstrates the sensitivity of the transport properties to the exact composition: 33×10^{-4} Ω cm and 75 μV/K[4], 22×10^{-3} Ω cm and 130 μV/K[7] and 40×10^{-3} Ω cm and 240 μV/K in this work. The difference between the transport properties of reported[4,7] and presently observed values can be explained on the basis of the non stoichiometry of the sample confirmed by the WDS.

Figure 6 displays the Seebeck coefficient S, as a function of temperature for all samples. The positive S-values evidence holes as the predominant charge carriers. S of all the samples increased with increasing temperature. The Cu-doped samples reveal an almost linear temperature dependence typically observed for metallic compounds. The Seebeck-coefficient at room temperature is systematically decreased with increasing nominal Cu-content, which may be due to the increase in carrier concentration by doping and it follows the Equation (1). The Equation (1) expresses the relationship between Seebeck coefficient and carrier concentration as

$$S_d\,(T > \theta_D) = \frac{\pi^2 k_B^2 2m_e}{e\hbar^2\left(3n\pi^2\right)^{2/3}}T \tag{1}$$

which describes the diffusion thermopower in terms of a free electron model,[21] with m_e being the electron mass, and e the carrier charge. As negative S values are observed for ZnSe (−178 to −370 μV/K between 300 K and 500 K for ZnSe thin film),[18] ZnSe has an adverse effect on the total S value because of negative charge carriers. Thus the total S value deceased because the presence of the electron dominant ZnSe phase in the hole dominant phase may suppress the thermoelectric voltage values due to their opposite charge carriers in the temperature gradient.

Figure 7 displays the temperature dependent thermal conductivity, λ (T), of all the samples. The electron contribution was calculated from the electrical resistivity applying the Wiedemann-Franz relation with a Lorentz number $L = 2.44 \times 10^{-8}$ W Ω K^{-2}. The remaining phonon part, λ_{ph}, is plotted in Fig. 7. The effect of ZnSe on thermal conductivity is rather due to the high thermal conductivity

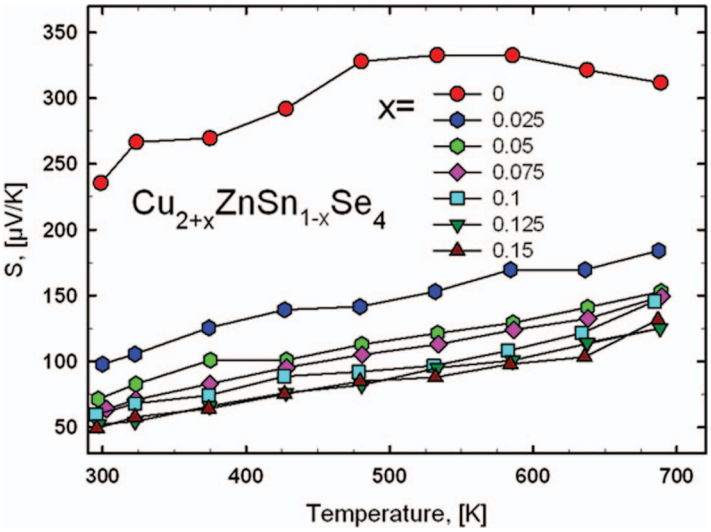

FIG. 6. Seebeck-coefficients of all samples $Cu_{2+x}ZnSn_{1-x}Se_4$ ($0 \leq x \leq 0.15$) as a function of temperature.

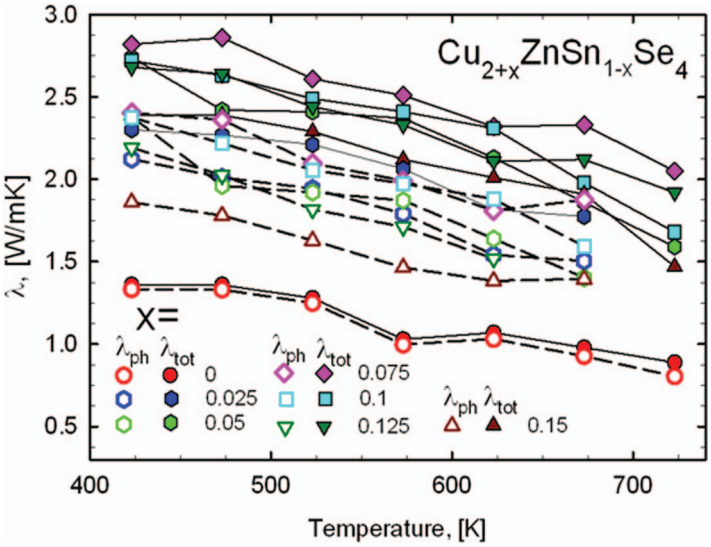

FIG. 7. Thermal conductivity as a function of temperature for $Cu_{2+x}ZnSn_{1-x}Se_4$ ($0 \leq x \leq 0.15$). The total thermal conductivity is displayed with filled symbols and the phonon contribution with open symbols.

value of ZnSe ($\lambda_{300K} = 19$ W m^{-1}K^{-1}).[17] The sample $Cu_2ZnSnSe_4$ exhibits by far the smallest total as well as phonon thermal conductivity. The increase of λ for all the other samples can be partially explained by the higher electronic contribution. The micrographs clearly show that the presence of ZnSe impurities ($\lambda_{300K} = 19$ W m^{-1} K^{-1})[17] in these samples is significantly higher than in $Cu_2ZnSnSe_4$, and thus a larger contribution of this phase to the overall thermal conductivity is expected. As Umklapp-processes dominate the scattering at high temperatures, a 1/T-dependence of λ_{ph} is found.

The thermoelectric figure of merit (zT) was evaluated from the power factor (PF), S^2/ρ, and the thermal conductivity (λ). The results for zT are plotted in Fig. 8 and show an increase as a function of temperature for all samples. Although the doping increased the power factor for all the samples with higher Cu-content, due to the significant rise of thermal conductivity, only the sample $Cu_{2.05}ZnSn_{0.95}Se_4$, which has an almost 2 times higher PF at 700 K compared to $Cu_2ZnSnSe_4$, exhibits improved values of zT. The maximum thermoelectric figure of merit reaches 0.3 at 720 K

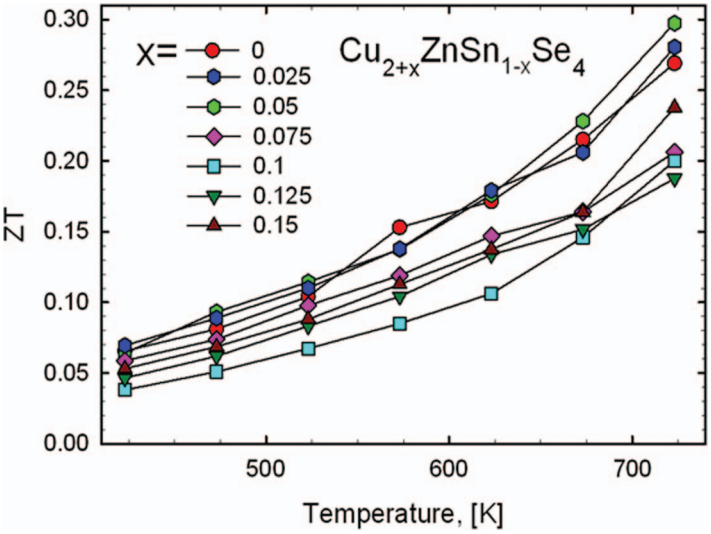

FIG. 8. Thermoelectric figure of merit, zT, as a function of temperature for $Cu_{2+x}ZnSn_{1-x}Se_4$ ($0 \leq x \leq 0.15$).

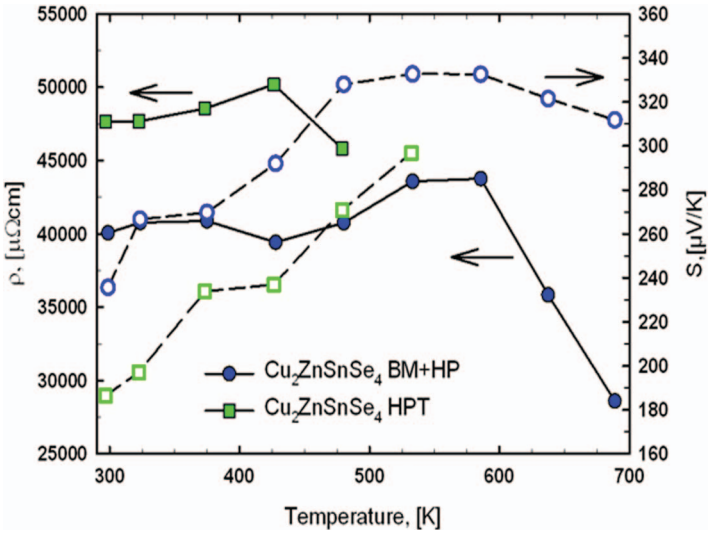

FIG. 9. Comparison of the electrical resistivity (full symbols) and the Seebeck-coefficient (open symbols) as a function of temperature for $Cu_2ZnSnSe_4$ before and after HPT.

for $Cu_{2.05}ZnSn_{0.95}Se_4$. The observed values are slightly smaller than in the literature reported for the uncoated bulk materials $Cu_{2.1}Zn_{0.9}SnSe_4$ (zT = 0.45 at 700 K),[4] and $Cu_2ZnSn_{0.9}In_{0.1}Se_4$ (zT = 0.37 at 700 K).[7] The presence of the ZnSe secondary phase, which is believed to show an adverse effect on transport properties, prevents a better thermoelectric performance.

C. Transport properties after high-pressure torsion (HPT)

As demonstrated for skutterudite compounds, severe plastic deformation created by HPT-treatment can lead to a significant improvement in the thermoelectric figure of merit. By lowering the average grain size, enhancement of the dislocation density and introducing additional defects in the crystal structure the thermal conductivity is decreased. As the unfavorable effect on the power factor is overcompensated by this reduction, an increased zT was observed.[22]

The samples $Cu_2ZnSnSe_4$ and $Cu_{2.05}ZnSn_{0.95}Se_4$ were exposed to the HPT process described in details in the experimental section. As expected, both samples show an increase of the electrical

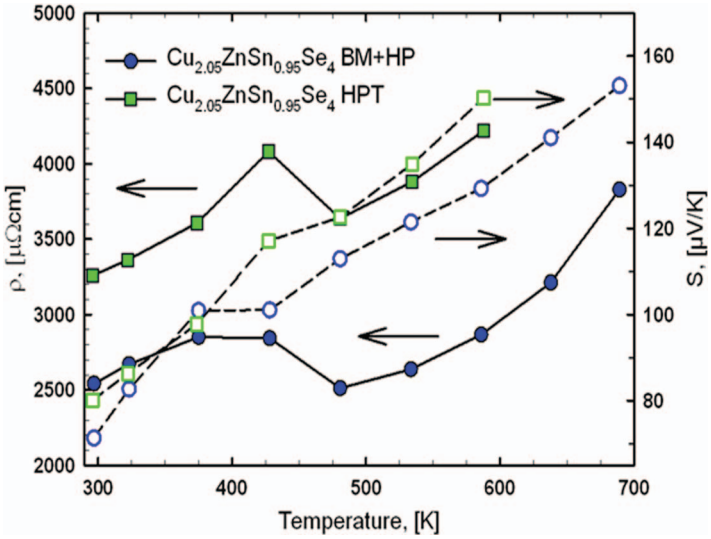

FIG. 10. Comparison of the electrical resistivity (full symbols) and the Seebeck- coefficient (Open symbols) as a function of temperature for $Cu_{2.05}ZnSn_{0.95}Se_4$ before and after HPT.

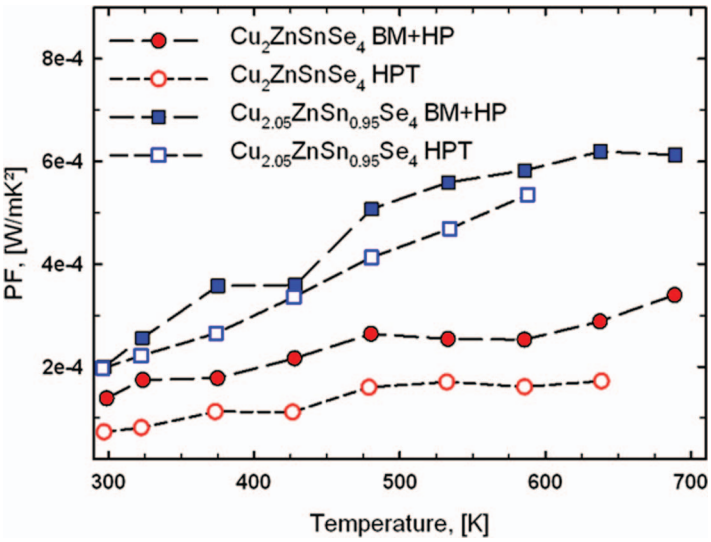

FIG. 11. Power factor of $Cu_2ZnSnSe_4$ and $Cu_{2.05}ZnSn_{0.95}Se_4$ as a function of temperature before (BM + HP, full symbols) and after HPT-treatment (open \symbols).

resistivity (Fig. 9 and 10), but in the case of $Cu_2ZnSnSe_4$ a decrease of the Seebeck coefficient was observed (Fig. 9), whereas S slightly increases for $Cu_{2.05}ZnSn_{0.95}Se_4$ (Fig. 10). As the HPT was carried out at 573 K small variations in composition are most likely the reasons for the change of the Seebeck-coefficients. In Fig. 11 the power factors (PF) of the two samples before and after high-pressure torsion are displayed. In both cases PF(T) after HPT is smaller, mainly due to the increase in electrical resistivity, but for $Cu_{2.05}ZnSn_{0.95}Se_4$ the marginal higher Seebeck coefficient is almost compensating the cutback of ρ.

The thermal conductivity of the HPT-treated samples at 420 K is decreased by ~30% in both cases, but with increasing temperature the difference to the ball milled and hot pressed samples is shrinking and expected to reach the same values around 700 K–750 K (Fig. 12). This observation leads to the conclusion that the introduced defects are already healing at these temperatures. Due to the reduced power factor accompanied by the moderate difference of λ no improvement of the

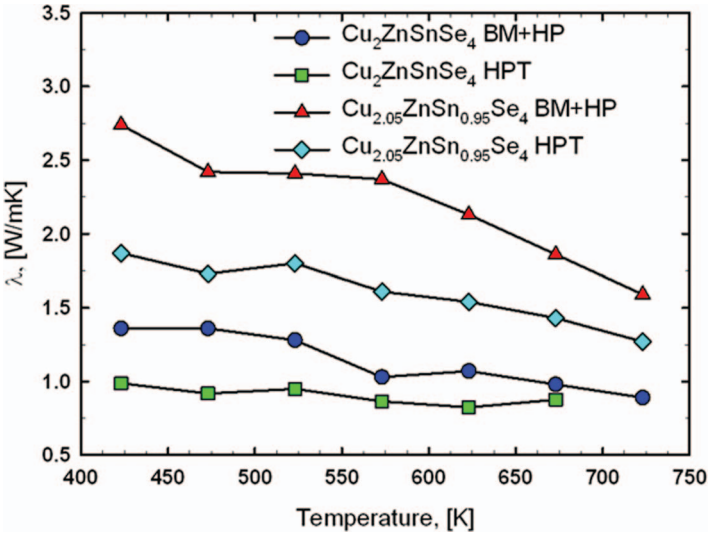

FIG. 12. Temperature dependent thermal conductivity of the two samples $Cu_2ZnSn_1Se_4$ and $Cu_{2.05}ZnSn_{0.95}Se_4$ before and after HPT.

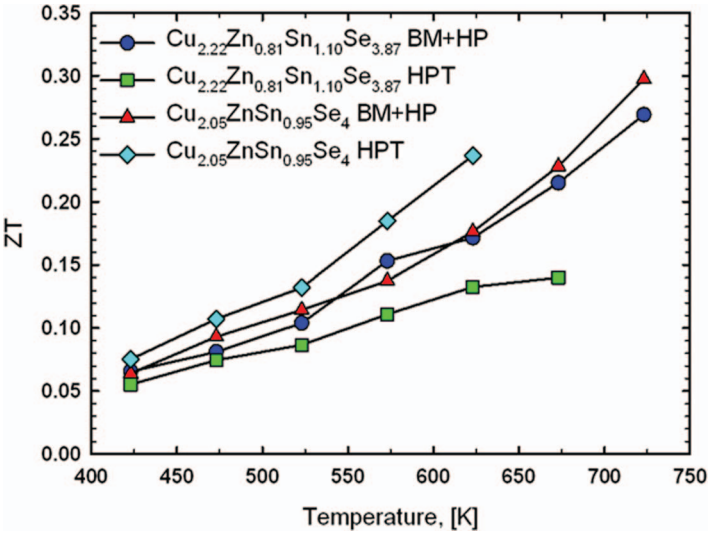

FIG. 13. Thermoelectric figure of merit, zT, of the two samples $Cu_2ZnSnSe_4$ and $Cu_{2.05}ZnSn_{0.95}Se_4$ before and after HPT as a function of temperature.

thermoelectric figure of merit zT for $Cu_2ZnSnSe_4$ is observed. In contrast to this, for $Cu_{2.05}ZnSn_{0.95}Se_4$ an improved thermoelectric performance up to 625 K is observed, where zT is increased by more than 30% mainly due to the decreased thermal conductivity (Fig. 13).

IV. CONCLUSIONS

The quaternary compounds $Cu_{2+x}ZnSn_{1-x}Se_4$ (x = 0, 0.025, 0.05, 0.75, 0.1, 0.125, 0.15) were synthesized by melting and annealing. The stannite phase with ZnSe as a secondary phase in all the samples was confirmed by Rietveld analysis of XRD patterns, WDS as well as Raman spectroscopy. In addition to these phases, the undoped and $Cu_{2+x}ZnSn_{1-x}Se_4$ (x = 0.125, 0.15) samples showed SnSe or CuSe as additional phases.

The temperature dependence of the electrical resistivity, the Seebeck coefficient and the thermal conductivity of samples $Cu_{2+x}ZnSn_{1-x}Se_4$ with $0 \leq x \leq 0.15$ were measured. The electrical

resistivity of all samples decreases with an increase of the doping level except for the sample $Cu_{2.1}ZnSn_{0.9}Se_4$ due to the presence of a higher content of ZnSe as a secondary phase (4.16 – 30.1 Ω cm at room temperature).[17] The positive Seebeck coefficient in all the samples documents that holes are the majority carriers. The smallest total as well as phonon thermal conductivity was observed for $Cu_2ZnSnSe_4$ with respect to the remaining doped samples. This may be attributed to the high content of the ZnSe phase ($\lambda_{300K} = 19$ W m^{-1} K^{-1}).[17] A dominant Umklapp scattering mechanism was found by the 1/T dependence of phonon thermal conductivity at elevated temperatures. The maximum $zT = 0.3$ was obtained for $Cu_{2.05}ZnSn_{0.95}Se_4$.

High-pressure torsion treatment resulted in an increase of the electrical resistivity and at the same time a significant reduction of the thermal conductivity. In case of $Cu_{2.05}ZnSn_{0.95}Se_4$ an improvement of the thermoelectric figure of merit at 625 K by more than 30% is observed.

ACKNOWLEDGMENTS

The authors would like to thank the Department of Science & Technology (DST), India for financial support through Grant No, INT/AUA/BMWF/P-13/2011 and the OEAD for support via the WTZ Austria-India under grant IN 09/2011.

[1] Matsushita, H., Takashi, M., Akinori, K., and Takeo, T, J. Cryst. Growth. **208**, 416–422 (2000).
[2] Nolas, G. S., Lin, X., Martin, J., Beekman, M., and Wang, H, J. Electron. Mater. **38**(7), 1052–1055 (2009).
[3] Slack G. A, *CRC Handbook of Thermoelectrics*, edited by Rowe D. M. (CRC, Boca Raton, 1995), p. 407.
[4] Liu, M.-L., Huang, F.-Q., Chen, L.-D., and Chen, I-W, Appl. Phys. Lett. **94**, 202103 (2009).
[5] Liu, M.-L., Chen, I-W., Huang, F.-Q., and Chen, L.-D, Adv. Mater. **21**, 3808–3812 (2009).
[6] C. H. L. GOODMAN, J. Phys. Chem. Solids Pergamon Press **6**, 305–314 (1958).
[7] Shi, X. Y., Huang, F. Q., Liu, M. L., and Chen, L. D, Appl. Phys. Lett. **94**, 122103 (2009).
[8] Zeier, W. G, Lalonde, A., Gibbs, Z. M., Heinrich, C. P., Panthöfer, M., Snyder, G. J., and Tremel, W., J. Am. Chem. Soc, **134**, 7147– 7154 (2012).
[9] Fan, F.-J., Yu, B., Wang, Y., Zhu, Y.-L., Liu, X.-J., Yu, S.-H., and Ren Z, J. Am. Chem. Soc. **133**(40) 15910–15913 (2011).
[10] Ibanez, M., Cadavid, D., Zamani, R., Garcia-Castello, N., Izquierdo-Roca, V., Li, W., Fairbrother, A., Prades, J. D., Shavel, A., Arbiol, J., Perez-Rodriguez, A., Morante, J. R., and Cabot A, Chem. Mater. **24**, 562–570 (2012).
[11] M. Ibanez, R. Zamani, A. LaLonde, D. Cadavid, W. H. Li, A. Shavel, J. Arbiol, J. R. Morante, S. Gorsse, G. J. Snyder, and A. Cabot, J. Am.Chem. Soc. **134**, 4060 (2012).
[12] Fan, F.-J., Wang, Y.-X., Liu, X.-J., Wu, L., and Yu, S.-H, Adv. Mater. **24**, 6158–6163 (2012).
[13] Roisnel, T., Rodriguez-Carvajal, J. Mater. Sci. Forum. **118**, 378–381 (2001).
[14] Goryunova, N. A., Kotovich, V. A., and Frank Kamenetskii, V. A, Doklady Akademii Nauk SSSR **103**, 659–662 (1955).
[15] M. Altosaar, J. Raudoja, K. Timmo, M. Danilson, M. Grossberg, J. Krustok, and E. Mellikov, Phys. Stat. Sol. a **205**(1), 167–170 (2008).
[16] Yamamoto, K. and Kashida, S, J.Solid St.Chem **93**, 202–211 (1991).
[17] O. Madelung, in *Semiconductors: Data Handbook*, 3rd Ed. (Springer, Berlin Heidelberg New York, 2004).
[18] B. K. Reddy, M. M. Reddy, R. Venugopal, and D. R. Reddy, Radiation Effects and Defects in Solids **145**, 133–142 (1998).
[19] S. Asanabe, J. Phys. Soc. Japan **14**, 281 (1959).
[20] Z. Ogorelic and D. Selinger, J.Mater.Sci **6**, 136–139 (1971).
[21] F. J. Blatt, *Physics of electronic conduction in solids*, p. 210 (McGraw-Hill, New York, 1968).
[22] G. Rogl, D. Setman, E. Schafler, J. Horky, M. Kerber, M. Zehetbauer, M. Falmbigl, P. Rogl, E. Royanian, and E. Bauer, Acta Materialia, **60**(5), 2146–2157 (2012).